

# EXPERIMENTAL DEMONSTRATION OF SYNERGY BETWEEN ELECTRON CYCLOTRON AND LOWER HYBRID CURRENT DRIVE ON TORE SUPRA

J.F. Artaud<sup>1</sup>, G. Giruzzi<sup>1</sup>, R.J. Dumont<sup>1</sup>, F. Imbeaux<sup>1</sup>, P. Bibet<sup>1</sup>, F. Bouquey<sup>1</sup>, J. Clary<sup>1</sup>, A. Ekedahl<sup>1</sup>, G.T. Hoang<sup>1</sup>, M. Lennholm<sup>1</sup>, R. Magne<sup>1</sup>, J.L. Ségui<sup>1</sup>, A. Bruschi<sup>2</sup>, G. Granucci<sup>2</sup>  
and the Tore Supra Team

1. Association EURATOM-CEA sur la Fusion, DSM / Département de Recherches sur la Fusion Contrôlée, CEA-Cadarache, 13108 St. Paul-lez-Durance (FRANCE)

2. Associazione EURATOM-ENEA sulla Fusione, IFP-CNR, Milano (ITALY)

## Introduction

Non-inductive current drive (CD) has two main applications in tokamaks: sustainment of a substantial fraction of the toroidal plasma current necessary for the plasma confinement and control of the plasma stability and transport properties by appropriate shaping of the current density profile. For the first kind of applications, lower hybrid (LH) waves are known to provide the highest efficiency (defined as the ratio of the driven current to the injected wave power), although with limited control capability. Conversely, electron cyclotron (EC) waves drive highly localized currents, and are therefore particularly suited for control purposes, but their CD efficiency is much lower than that of LH waves (typically, an order of magnitude in present day experiments). The reason for this difference is related to the different interaction mechanisms of the two waves with the electrons: parallel velocity diffusion associated with Landau damping for LH waves and perpendicular velocity diffusion associated with cyclotron damping for EC waves (parallel and perpendicular directions are defined with respect to the tokamak magnetic field). LH waves can efficiently interact with electrons with substantially higher parallel velocities, poorly collisional and insensitive to trapping, thus carrying a larger current than the slower electrons interacting with the EC waves. For these reasons, the idea of combining the two CD systems has been proposed and investigated since the early '80s theoretically [1] and experimentally [2,3,4,5,6]. Moreover, various calculations [7,8,9] have demonstrated an interesting property: the current driven by the simultaneous use of the two waves,  $I_{LH+EC}$ , can be significantly larger than the sum  $I_{LH}+I_{EC}$  of the currents separately driven by the two waves in the same plasma conditions. This property, hereafter called synergy effect. Early experiments tried to demonstrate this effect, but were inconclusive [5,6]. Effective coupling of up-shifted and down-shifted EC waves with the LH driven electron tail has been observed in FTU in a qualitative way, due to the lower effects on current at the higher densities involved [10]. Therefore, so far a well documented qualitative and quantitative experimental demonstration of the synergy effect in steady state was missing. Here, the first experimental demonstration of this type is reported.

## LHCD + ECCD in Tore Supra

An unambiguous experimental demonstration of the synergy effect requires: 1) stationary conditions, i.e., constant  $I_p$ , constant density and no substantial electric field effects; 2)

good confinement of the current carrying electrons; 3) large optical depth of the EC waves. If all these conditions are met, not only a qualitative assessment, but also a quantitative comparison with the CD improvement predicted by kinetic theory is possible. The synergy effect can be quantified, e.g., by the synergy factor [8], defined as  $F_{\text{SYN}} = \Delta I / I_{\text{EC}}$ , where  $\Delta I = I_{\text{LH+EC}} - I_{\text{LH}}$  is the additional EC current driven in the presence of LH waves. Dedicated experiments have been performed in the Tore Supra tokamak (major radius  $R = 2.40$  m, minor radius  $a = 0.72$  m, magnetic field  $B = 3.8$  T, circular cross-section). Discharges of a duration of 30 s were realized in deuterium, at a plasma current  $I_p = 0.58$  MA, central electron density  $n_{e0} = 1.8 \cdot 10^{19} \text{ m}^{-3}$ , central electron temperature  $T_{e0} = 6 - 8$  keV, central ion temperature  $T_{i0} = 1.7$  keV, effective ion charge  $Z_{\text{eff}} = 4$ . After an initial Ohmic phase, the transformer flux was kept constant and current was generated by LH waves, launched by two couplers with power spectra peaked at  $n_{\parallel} = 2$  and a total power of the order of  $P_{\text{LH}} = 3$  MW. Calculated bootstrap current contribution was of the order of  $I_b / I_p = 10\text{-}15\%$ . A multiple feedback strategy was employed, with the following actuators: 1) gas puff to keep the plasma density constant; 2) LH power to keep the plasma current constant; 3) transformer flux to keep the loop voltage  $V_{\text{loop}}$  constant and exactly equal to zero. On the stationary phase of this target plasma, EC waves have been injected for a duration of 10 s. Two gyrotrons [11] have been used, for a total power injected into the plasma  $P_{\text{EC}} = 0.7$  MW (in the ordinary mode). Toroidal angles have been varied, by means of poloidally and toroidally steerable mirrors, in the range  $+20^\circ - +28^\circ$ , in order to drive currents in the same direction as the LH current. Various combinations of poloidal and toroidal angles of the two mirrors have been used to change the radial location of the EC driven current. During the ECCD phase, the LH power is expected to drop by an amount  $\Delta P_{\text{LH}}$ , because the plasma current is kept constant. Since the loop voltage is zero, this drop is easily translated into the corresponding additional current  $\Delta I$ , driven by the EC waves in the presence of LH waves, by the formula:  $\Delta I = (I_p - I_{\text{BS}}) \Delta P_{\text{LH}} / P_{\text{LH}}$  (1).

This current is then compared to the current  $I_{\text{EC}}$  that would be driven by ECCD alone in the same plasma conditions, which can be evaluated by means of standard toroidal ray-tracing codes, coupled to a Fokker-Planck code or, more simply, to linear expressions of the current drive efficiency derived with the adjoint formalism and including electron trapping effects [12], which is completely appropriate to the power level used in these experiments.

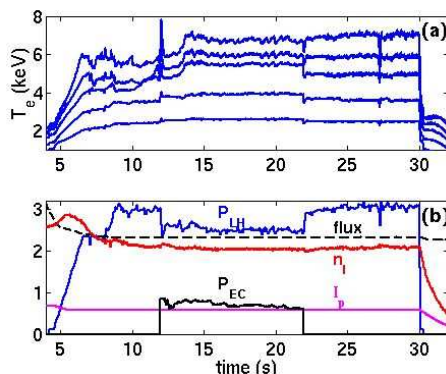


Fig. 1: Tore Supra discharge 31463. (a) Electron temperature measured by ECE at various plasma positions, covering the region  $0 \leq r/a \leq 0.4$ . (b) From top to bottom, as a function of time, LH power (MW), transformer flux (Wb), line integrated density ( $10^{19} \text{ m}^{-2}$ ), EC power (MW) and plasma current (MA).

The key point is that these theoretical expressions have been fully validated by dedicated series of experiments, performed on DIII-D in a variety of different plasma conditions [13]: they can be used as a reliable reference for the ECCD efficiency in conditions of strong single pass absorption and good confinement of the current carrying electrons. The results obtained are well illustrated by the time history of discharge 31463, shown in Fig. 1. During the application of ECCD ( $P_{\text{EC}} = 0.7$  MW), the LH power drops by approximately  $\Delta P_{\text{LH}} \approx 0.5$  MW, at constant transformer flux, plasma current and density. This simple experimental fact implies that the additional current driven by the ECCD has an efficiency of the same order of magnitude as LHCD.

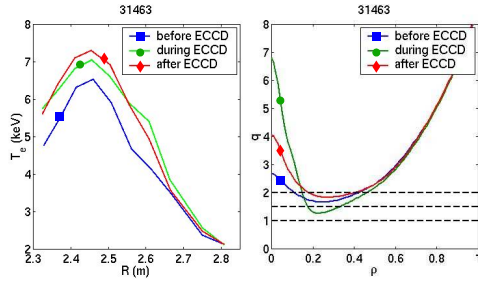


Fig. 2: electron temperature profiles (from ECE) versus major radius coordinate  $R$  and  $q$  profile (reconstructed by the CRONOS code) versus normalised radius, for discharge 31463.

hard X-ray profile, measured by means of a 38 lines-of-sight camera, does not substantially change during the ECCD phase, with respect to both the pre-ECCD and the post-ECCD phases. The large drop of  $P_{LH}$  in the ECCD phase can not be explained by an increase of

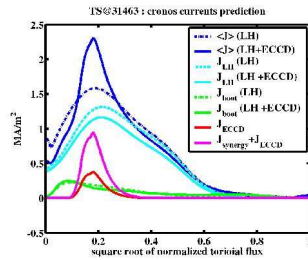


Fig. 3: currents profiles versus normalised radius, from CRONOS simulation : we can see very small change in bootstrap current profile and in LH profile shape between LH phase and LH + ECCD phase. The ECCD current is computed with ray tracing + adjoint theory .

the LHCD efficiency due to the temperature increase. In fact, the  $P_{LH}$  level is the same in the pre- and the post-ECCD phase, in which  $T_e$  has different values: this means that the LHCD efficiency is weakly dependent on  $T_e$  in this temperature range. Note that this temperature difference before and after the ECCD phase is due to a change in the confinement properties of the discharge, related to a corresponding change in the  $q$  profile, as shown in Fig. 2. The little change of the  $T_e$  profile from the ECCD phase to the post-ECCD phase also explains why the bootstrap current changes little (Fig. 3). Variations of the LH wave coupling are also  $< 3\%$ . Therefore, the synergy effect remains the most plausible explanation of the ECCD efficiency improvement. The radial location  $\rho_{EC}$  at which the EC current is driven has then been varied by changing the poloidal and toroidal launch angles (Fig. 4), and it has been observed that the synergy effect depends on this location. The measured additional currents  $\Delta I$  and the linear ECCD currents  $I_{EC}$  are shown in Fig. 5. The error bars of  $\Delta I$  correspond to the standard deviation associated with the statistical variations of  $P_{LH}$  and  $I_{bs}$  (calculated from the measured plasma parameters by means of the NCLASS code [15] and CRONOS code [16]) in the time intervals chosen for the analysis. The error bars of  $I_{EC}$  also correspond to statistical variations of the measured plasma parameters and, in addition, to the uncertainty on the injection angles ( $\pm 1^\circ$ , typically). The estimate of  $\Delta I$  can be corrected by smaller effects due to other parameters (slight  $I_p$ ,  $n_e$  and  $Z_{eff}$  variations,

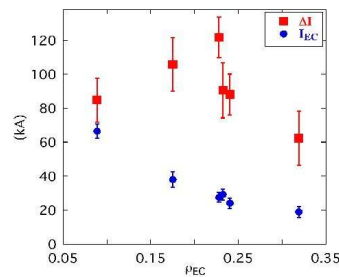


Fig. 5: Measured additional current driven by ECCD in the presence of LHCD (squares) and computed ECCD current (dots) versus the location (in normalized radius) of maximum EC power deposition (computed).

Application of Eq. (1), with a computed bootstrap current  $I_{BS} \approx 90$  kA, yields  $\Delta I \approx 90$  kA, to be compared with  $I_{EC} \approx 24$  kA, computed by means of a toroidal ray-tracing code [14] using the measured plasma parameters and antenna geometry, and including the linear ECCD computation by the adjoint formalism [14]. In this case, the toroidal injection angles of the two EC wave beams were  $24^\circ$ , and the poloidal injection angles had been chosen in order to drive a current peaked at the same location as the LH driven current. In fact, the

hard X-ray profile, measured by means of a 38 lines-of-sight camera, does not substantially change during the ECCD phase, with respect to both the pre-ECCD and the post-ECCD phases. The large drop of  $P_{LH}$  in the ECCD phase can not be explained by an increase of the LHCD efficiency due to the temperature increase. In fact, the  $P_{LH}$  level is the same in the pre- and the post-ECCD phase, in which  $T_e$  has different values: this means that the LHCD efficiency is weakly dependent on  $T_e$  in this temperature range. Note that this temperature difference before and after the ECCD phase is due to a change in the confinement properties of the discharge, related to a corresponding change in the  $q$  profile, as shown in Fig. 2. The little change of the  $T_e$  profile from the ECCD phase to the post-ECCD phase also explains why the bootstrap current changes little (Fig. 3). Variations of the LH wave coupling are also  $< 3\%$ . Therefore, the synergy effect remains the most plausible explanation of the ECCD efficiency improvement. The radial location  $\rho_{EC}$  at which the EC current is driven has then been varied by changing the poloidal and toroidal launch angles (Fig. 4), and it has been observed that the synergy effect depends on this location. The measured additional currents  $\Delta I$  and the linear ECCD currents  $I_{EC}$  are shown in Fig. 5. The error bars of  $\Delta I$  correspond to the standard deviation associated with the statistical variations of  $P_{LH}$  and  $I_{bs}$  (calculated from the measured plasma parameters by means of the NCLASS code [15] and CRONOS code [16]) in the time intervals chosen for the analysis. The error bars of  $I_{EC}$  also correspond to statistical variations of the measured plasma parameters and, in addition, to the uncertainty on the injection angles ( $\pm 1^\circ$ , typically). The estimate of  $\Delta I$  can be corrected by smaller effects due to other parameters (slight  $I_p$ ,  $n_e$  and  $Z_{eff}$  variations,

Application of Eq. (1), with a computed bootstrap current  $I_{BS} \approx 90$  kA, yields  $\Delta I \approx 90$  kA, to be compared with  $I_{EC} \approx 24$  kA, computed by means of a toroidal ray-tracing code [14] using the measured plasma parameters and antenna geometry, and including the linear ECCD computation by the adjoint formalism [14]. In this case, the toroidal injection angles of the two EC wave beams were  $24^\circ$ , and the poloidal injection angles had been chosen in order to drive a current peaked at the same location as the LH driven current. In fact, the

hard X-ray profile, measured by means of a 38 lines-of-sight camera, does not substantially change during the ECCD phase, with respect to both the pre-ECCD and the post-ECCD phases. The large drop of  $P_{LH}$  in the ECCD phase can not be explained by an increase of the LHCD efficiency due to the temperature increase. In fact, the  $P_{LH}$  level is the same in the pre- and the post-ECCD phase, in which  $T_e$  has different values: this means that the LHCD efficiency is weakly dependent on  $T_e$  in this temperature range. Note that this temperature difference before and after the ECCD phase is due to a change in the confinement properties of the discharge, related to a corresponding change in the  $q$  profile, as shown in Fig. 2. The little change of the  $T_e$  profile from the ECCD phase to the post-ECCD phase also explains why the bootstrap current changes little (Fig. 3). Variations of the LH wave coupling are also  $< 3\%$ . Therefore, the synergy effect remains the most plausible explanation of the ECCD efficiency improvement. The radial location  $\rho_{EC}$  at which the EC current is driven has then been varied by changing the poloidal and toroidal launch angles (Fig. 4), and it has been observed that the synergy effect depends on this location. The measured additional currents  $\Delta I$  and the linear ECCD currents  $I_{EC}$  are shown in Fig. 5. The error bars of  $\Delta I$  correspond to the standard deviation associated with the statistical variations of  $P_{LH}$  and  $I_{bs}$  (calculated from the measured plasma parameters by means of the NCLASS code [15] and CRONOS code [16]) in the time intervals chosen for the analysis. The error bars of  $I_{EC}$  also correspond to statistical variations of the measured plasma parameters and, in addition, to the uncertainty on the injection angles ( $\pm 1^\circ$ , typically). The estimate of  $\Delta I$  can be corrected by smaller effects due to other parameters (slight  $I_p$ ,  $n_e$  and  $Z_{eff}$  variations,

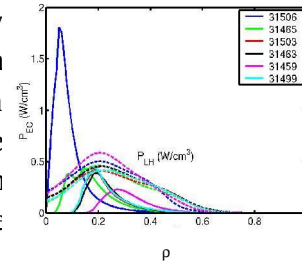


Fig. 4: for each shot, LH current profile deduced from hard X measurement and ECCD current profile calculate with ray tracing + adjoint theory

measured additional currents  $\Delta I$  and the linear ECCD currents  $I_{EC}$  are shown in Fig. 5. The error bars of  $\Delta I$  correspond to the standard deviation associated with the statistical variations of  $P_{LH}$  and  $I_{bs}$  (calculated from the measured plasma parameters by means of the NCLASS code [15] and CRONOS code [16]) in the time intervals chosen for the analysis. The error bars of  $I_{EC}$  also correspond to statistical variations of the measured plasma parameters and, in addition, to the uncertainty on the injection angles ( $\pm 1^\circ$ , typically). The estimate of  $\Delta I$  can be corrected by smaller effects due to other parameters (slight  $I_p$ ,  $n_e$  and  $Z_{eff}$  variations,

Application of Eq. (1), with a computed bootstrap current  $I_{BS} \approx 90$  kA, yields  $\Delta I \approx 90$  kA, to be compared with  $I_{EC} \approx 24$  kA, computed by means of a toroidal ray-tracing code [14] using the measured plasma parameters and antenna geometry, and including the linear ECCD computation by the adjoint formalism [14]. In this case, the toroidal injection angles of the two EC wave beams were  $24^\circ$ , and the poloidal injection angles had been chosen in order to drive a current peaked at the same location as the LH driven current. In fact, the

transient Ohmic current, weak dependence of  $I_{LH}$  on  $T_e$ , LH coupling variation during the ECCD phase). These corrections moderately affect the mean value of  $\Delta I$  and of its error bar, but do not change the overall conclusion:  $\Delta I$  is always larger than  $I_{EC}$ .

### Comparison with kinetic theory

The dependence of  $\Delta I$  on  $\rho_{EC}$  (or on the launching angles) is not easy to understand. To this end, kinetic simulations of the discharges presented in Fig. 5 have been performed, using a 3-D Fokker Planck code [16]. Reproducing the driven currents both in the LH and LH+EC phases is a difficult task, which depends on details of the LH spectrum inside the plasma. Here, a model LH spectrum that reproduces the overall features of the measured hard X-ray profiles is used, and the comparison is focused on the synergy factor  $F_{syn}$ . The measured temperature and density profiles as well as other experimental parameters are used as an input to the Fokker-Planck code. The EC wave beam propagation is described by tracing 150 rays per beam and summing up all the contributions to the quasilinear diffusion coefficient. The result of the comparison of the synergy factors for the discharges of Fig. 3 is shown in Fig. 6. The overall behaviour of the synergy factor as a function of  $\rho_{EC}$  is well reproduced, in particular the strong reduction for central EC power deposition. This is mainly due to the fact that the LH power deposition is hollow. Note, however, that the overlap in space of the power deposition of the two waves, although a necessary condition for the synergy effect, is not a sufficient one. Overlap in velocity space of the two interactions is also necessary [9].

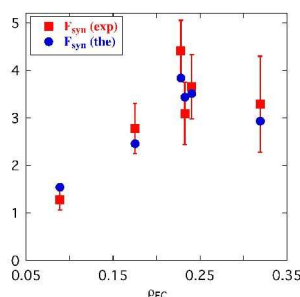


Fig. 6: synergy factors from experiment and from kinetic theory

### Conclusion

In conclusion, the peculiar experimental conditions attainable on the Tore Supra tokamak have allowed the first experimental demonstration of the synergy between EC and LH current drive. The significant improvement of the ECCD efficiency in the presence of LHCD, predicted by kinetic theory and confirmed by stationary experiments on Tore Supra, opens up the possibility of using ECCD as an efficient current profile control tool in LHCD plasmas.

### References

- [1] I. Fidone et al., Phys. Fluids **27**, 2468 (1984).
- [2] A. Ando et al., Phys. Rev. Lett. **56**, 2180 (1986); A. Ando et al., Nucl. Fusion **26**, 107 (1986).
- [3] T. Yamamoto et al., Phys. Rev. Lett. **58**, 2220 (1987); H. Kawashima et al., Nucl. Fusion **31**, 495 (1991).
- [4] T. Maekawa et al., Phys. Rev. Lett. **70**, 2561 (1993); T. Maehara et al., Nucl. Fusion **38**, 39 (1998).
- [5] J. A. Colborn et al., Nucl. Fusion **38**, 783 (1998).
- [6] C. Côté et al., 25th EPS Conf. on Contr. Fusion and Plasma Phys., Praha, **22C**, 1336, (1998).
- [7] I. Fidone et al., Nucl. Fusion **27**, 579 (1987).
- [8] R.J. Dumont et al., Phys. Plasmas **7**, 4972 (2000).
- [9] R.J. Dumont and G. Giruzzi, Phys. Plasmas **11**, 3449 (2004).
- [10] G. Granucci et al., 12th Joint Workshop on ECE and ECRH, World Scientific, Singapore, (2003), 341.
- [11] M. Lennholm et al., Nucl. Fusion **43**, 1458 (2003).
- [12] R. H. Cohen, Phys. Fluids **30**, 2442 (1987).
- [13] C. C. Petty et al., Nucl. Fusion **42**, 1366 (2002).
- [14] V. Krivenski et al., Nucl. Fusion **25**, 127 (1985).
- [15] W.A. Houlberg et al., Phys. Plasmas **4**, 3230 (1997).
- [16] G. Giruzzi, Plasma Phys. Contr. Fusion **35**, A123 (1993).
- [17] V. Basiuk et al., Nucl. Fusion, **43** (2003) 822